Ecotoxicology and Environmental Safety 234 (2022) 113391

Contents lists available at ScienceDirect

Ecotoxicology and Environmental Safety

journal homepage: www.elsevier.com/locate/ecoenv

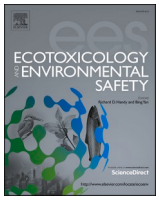

A highly parallel DTT/MB-DNA/Au electrochemical biosensor for trace Hg monitoring by using configuration occupation approach and SECM

Dandan Kong [a,*], Xinyue Li [a], Yang Tang [b], Ming Sui [a], Jinping Li [c], Yonggui Ma [c], Gaofeng Wang [a,c], Wei Gu [a,c], Xuegang Guo [c], Meihua Yang [a,*]

[a] Key Laboratory of Bioactive Substances and Resources Utilization of Chinese Herbal Medicine, Ministry of Education, Institute of Medicinal Plant Development, Chinese Academy of Medical Sciences & Peking Union Medical College, Beijing 100193, PR China
[b] Institute of Applied Electrochemistry, Beijing University of Chemical Technology, Beijing 100029, PR China
[c] Academy of Plateau Science and Sustainability, Qinghai Normal University / Key Laboratory of medicinal animal and plant resources of Qinghai Tibet Plateau, Xining, Qinghai 810008, PR China

ARTICLE INFO

Edited By: Guorui Liu(CGUOL)

Keywords:
DTT/MB-DNA/Au
Hg
Steric-hinerance effect
SECM
Plants and medical products

ABSTRACT

Environmental pollution and medicine safety have aroused increasing public concerns due to human health. Amongst various contaminants, mercury is of special attention owing to their environmental persistence and biogeochemical recycling and ecological risks. Herein, a simple and highly parallel electrochemical biosensor for Hg determination was designed and investigated. The proposed biosensor was prepared and compared between (1) DTT/MB-DNA/Au with configuration occupation approach and (2) MCH/MB-DNA/Au with passivation approach. According to the combined results of scanning electrochemical microscope (SECM) and Randles-Sevcik equation, the DTT modified electrode exhibited high uniformity on DNA distribution and superb stability on electron transfer in Hg^{2+} detection. Evidentially, the response value of proposed DTT/MB-DNA/Au was increased from 57.518% to 97.607%, while RSD% between duplicate runs had dropped from 22.658% to 0.223% (n = 3). Moreover, the increased proportion of effective working area was 467.380% compared with general sensors. Besides, DTT concentration, DNA concentration as well as assembly time were optimized, utilizing electrochemical impedance spectroscopy (EIS), Cyclic Voltammetry (CV) and Square Wave Anode Stripping Voltammetry (SWASV). This optimized biosensor exhibited an excellent selectivity toward Hg^{2+} over Cu^{2+}, As^{2+}, Cd^{2+}, Pb^{2+}, Cr^{3+}, Ni^{2+} and Zn^{2+} etc., and the stability of DTT/MB-DNA/Au were at least two times better even after 3 days under room temperature. Also, a linear relation was observed between the peak current and Hg^{2+}concentrations in a range from 0.25 nM to 2.00 μM with a detection limit of 53.00 pM under optimal conditions. Finally, DTT/MB-DNA/Au was applied for plants and medical products analysis. In all, this optimized DTT/MB-DNA/Au with advantages of high repeatability and sensitivity would provide a new insight into the design and application of biosensor for reliable sensing in safeguarding plant protection and medicinal safety.

1. Introduction

Mercury ion (Hg^{2+}) is considered highly toxic even at trace level, which can harm human organs and thereby lead to nervous breakdown, stomach disorder, heart diseases and kidneys failure (He et al., 2019; Liu et al., 2020; Sinaei et al., 2018). Due to its environmental persistence and bioaccumulation nature, trace Hg could readily enter plants, food chain and adversely affects human health (Fitzgerald et al., 2007; Clarkson and Magos, 2006). In consideration of these risks, the precise and fast screen of trace Hg has become one of the biggest challenges when it comes to effective controlling of Hg pollution and safeguarding the environment and human safety (Liang et al., 2021; Wang et al., 2021a, 2021b, 2021c). Up to now, numerous well developed Hg analysis methods have been reported and commercialized, such as inductively coupled plasma mass spectrometer (ICP-MS), atomic absorption spectroscopy (AAS), high performance liquid chromatography (HPLC) and x-ray florescence (XRF), etc. (Dmitry et al., 2022; Elisabeth et al., 2018; Fernanda et al., 2019; Konstantin et al., 2018; F. Li et al., 2021; J. Li et al., 2021; Tamara et al., 2022; Timmaraju et al., 2016). Although the above-mentioned methods have a high priority on sensitivity and

* Corresponding authors.
E-mail addresses: k_dandan@163.com (D. Kong), yangmeihua15@hotmail.com (M. Yang).

https://doi.org/10.1016/j.ecoenv.2022.113391
Received 20 August 2021; Received in revised form 22 February 2022; Accepted 3 March 2022
Available online 11 March 2022

accuracy, they do not applicate as a convenient portable analysis instrument for frequent use, mainly due to the expensive price and strict operation requirements. Meanwhile, a variety of fast screening systems have been reported for detecting Hg in water, soil and food-related products (Sapari et al., 2020; Yu et al., 2021; Marinho et al., 2020), including Elisa strip, immunochromatographic method, metal complexation chromogenic method, surface plasmon resonance, fluorescence and electrochemical sensors (Zhou et al., 2013; Zhang et al., 2017; Martinis and Wuilloud, 2016; Wang et al., 2020; Do Nascimento and Masini, 2012). Among all types of electrochemical sensors, DNA based electrochemical biosensor held important research value in the field of rapid detection of environmental pollutants owing to its intrinsic superiority of miniaturization, fast response, high sensitivity and specificity (Zhang et al., 2016; Liu et al., 2020; Hai et al., 2020). However, few DNA based electrochemical biosensor can be further applied in plants or medical products, which are mainly limited by the uncertain differences between batches, the interference substances in complex matrix and harsh conditions of preservation (Wang et al., 2021a, 2021b, 2021c; Sanz et al., 2021; Kong et al., 2020). Moreover, the researches aimed to minimize the differences between batches and increase the stability in complex have focused on the electrode interface modification process (Bonciu et al., 2021; Himori et al., 2021). On the contrary, the assembly mechanism of DNA sequence on electrode interface was rarely addressed in the literatures.

The primary goal of this study is to establish a simple and highly parallel electrochemical biosensor for the analysis of trace Hg in plants and medicinal products with low batch difference, high stability and outstanding sensitivity. For this purpose, a complementary investigation was initiated from the design and preparation of DNA biosensor with two different blocking chemical compounds, DTT/MB-DNA/Au with configuration occupation approach and MCH/MB-DNA/Au with passivation approach (Jia et al., 2015; Wang et al., 2014; Liu et al., 2021; Yu et al., 2019). Subsequently, the spatial structure and distribution of DNA sequence on Au interface was characterized by Scanning electrochemical microscope (SECM), and the effective current response was explained by Randles-Sevcik equation (Kong et al., 2020; Krukiewicz et al., 2018; Henstridge et al., 2012), electrochemical impedance spectroscopy (EIS), Cyclic Voltametry (CV) and Square Wave Anode Stripping Voltammetry (SWASV). Besides, the methodological investigation was carried out after the optimization of assembly condition. Finally, DTT/MB-DNA/Au was applied to the rapid analysis of trace Hg in plants and medicinal products. This study has provided a significant reference and guidance on the smart design and application of electrochemical biosensor with low batch differences, high stability and sensitivity, in the field of safeguarding plant protection and medicinal safety.

2. Material and methods

2.1. Apparatus and chemicals

All electrochemical measurements were performed with an Electrochemistry Workstation coupled with Scanning Electrochemical Microscope (SECM, Versa STAT 3 F Ametek, America). SECM studies were undertaken in electrode substrate feedback mode at constant height using Pt ultra-microelectrode (UME) in 2.00 mM $[Fe(CN)_6]^{3-}$, where the substrate was held at constant potential of 0.25 V with a electrochemistry workstation to construct a potentiostatic curve. A 10.0 μm Pt UME was used as a tip, and was positioned approximately 100.0 μm above the electrode surface, using standard methods for surface approach with $[Fe(CN)_6]^{3-}$ mediator solution while the electrode substrate was polarized at 0.25 V to ensure positive feedback, and was later flushed with H_2SO_4 solution before each SECM experiment. A traditional three electrodes system was adopted with Hg/Hg_2Cl_2 electrode (Saturated calomel electrode, SCE) as the reference electrode and a platinum plate as the auxiliary electrode, and a bare Au electrode (AuE, 3.0 mm in diameter) was employed as the substrate of modifying DNA due to its stability and specifically adsorption capacity with sulfhydryl group. All the aqueous solutions were prepared with deionized water (R=18.20 MΩ cm at 25.0 °C) obtained by a Millipore Milli-Q system (Millipore, Molsheim, Francia). The digestion was carried out using a Berjghof microwave system (Speedwave-3 +, Berjghof, Germany).

The single- stranded DNA (5′-HS-$(CH_2)_6$-TTTTTTTTTTTT-$(CH_2)_6$-Methylene blue-3′) was HPLC-purified and obtained from Sangon Biotechnology Co., Ltd. (Shanghai, China). Dithiothreitol (DTT), 6-mercapto-1-hexanol (MCH), tris (2-carboxyethyl) phosphine hydrochloride (TCEP), ethylene diamine tetra-acetic acid (EDTA) were purchased from Aladdin Biochemical Technology Co., Ltd (Shanghai, China). The buffer solution contained 0.10 M Tris-HCl (pH 7.40, 0.10 M NaCl and 5.00 mM $MgCl_2$), 10.00 mM TE (pH 8.00, 1.00 mM EDTA, 10.00 mM Tris-HCl), 10.00 mM Tris-HCl (pH 7.40, 20.00 mM TCEP, and 1.00 M NaCl), 10 mM phosphate buffer solution (PBS, pH 7.40, 0.50 M NaCl, 2.70 mM KCl). A DNA solution of 100.00 μM was prepared by centrifuging the tube containing sulfhydryl DNA lyophilized powder at 4000 r for 5 min and adding 186.00 μL 10.00 mM TE buffer (10.00 mM Tris-HCl and 1.00 mM EDTA). The DNA solution of 100.00 μM was diluted to 20.00 μM with 10.00 mM Tris-HCl buffer (1.00 mM TCEP) and then packed into different centrifugation tubes and stored at − 20 ℃. The standard solutions of Hg, As, Cu, Cd, Cu, Pb, Zn, Ni and Cr were purchased from National Institute of Metrology (P.R. China) and diluted as required. All the other reagents mentioned were analytical reagent grades and used without further purification.

2.2. Sample preparation

The plant and medicinal product samples of Astragalus membranaceus, Cassia stem and a regular medicinal formulation decoction were collected from local pharmacy in Beijing, China. The original concentrations of Hg in medicinal samples were confirmed by ICP-MS, which are 1.0 $nmol.L^{-1}$ in Astragalus membranaceus, 1.10 $nmol.L^{-1}$ in Cassia stem and 2.05 $nmol.L^{-1}$ in regular medicinal formulation, respectively. All the medicinal samples were dried until a constant weight was obtained in oven at 80 °C, and the dried samples were powdered with a stainless steel blender and stored at 4 °C in plastic bags for electrochemical analysis (Ajjabi and Chouba, 2009; Wang et al., 2018a, 2018b; García-Seoane et al., 2019; Yan et al., 2020;). For real samples analysis, samples of plants and medicinal products (0.50 g) were accurately weighted and digested with the mixed solution of 8.57 mL of HNO_3 and 1.43 mL H_2O_2 (6:1, *v/v*) in microwave digestion system for 10 h, and then was totally digested according to the published articles (Kong et al., 2020; Meng et al., 2017). All samples were spiked with different concentration of Hg and the analytical determination was performed with the standard additions method. The digested sample solutions were filtered with micro-filtration membrane (0.45 μm) and diluted to 50.00 mL flask with ultrapure water (Pinheiro et al., 2019; He et al., 2018).

2.3. DNA/DTT-AuE preparation and characterization

2.3.1. DNA/DTT-AuE preparation

The Au electrode was polished on alumina powders (1.00, 0.30, and 0.05 μm in diameter) until the surface was smooth, sonicated in ethanol and ultra-pure water (each for 2 min) and then rinsed with ethanol and dried in a stream of nitrogen [20]. Subsequently, the AuE is electrochemical cleaned by cyclic voltammetry (CV) between − 0.20 V and 1.50 V (vs. SCE) at 0.05 $V.s^{-1}$ in H_2SO_4 until obtained a steady redox wave (Fig. S1). Finally, the AuE was rinsed with ultrapure water and dried with nitrogen. The biosensor was prepared by two different blocking chemical compounds of DTT or MCH. For the configuration occupation approach with DTT, the cleaned electrode was first immersed in 200.00 μL of 100.00 μM freshly prepared DTT solution (dissolved in 10.00 mM Tris-HCl and 1.00 M NaCl) for 10 min, and then the DTT modified electrode was immersed in 10.00 μL of 1.00 μM DNA

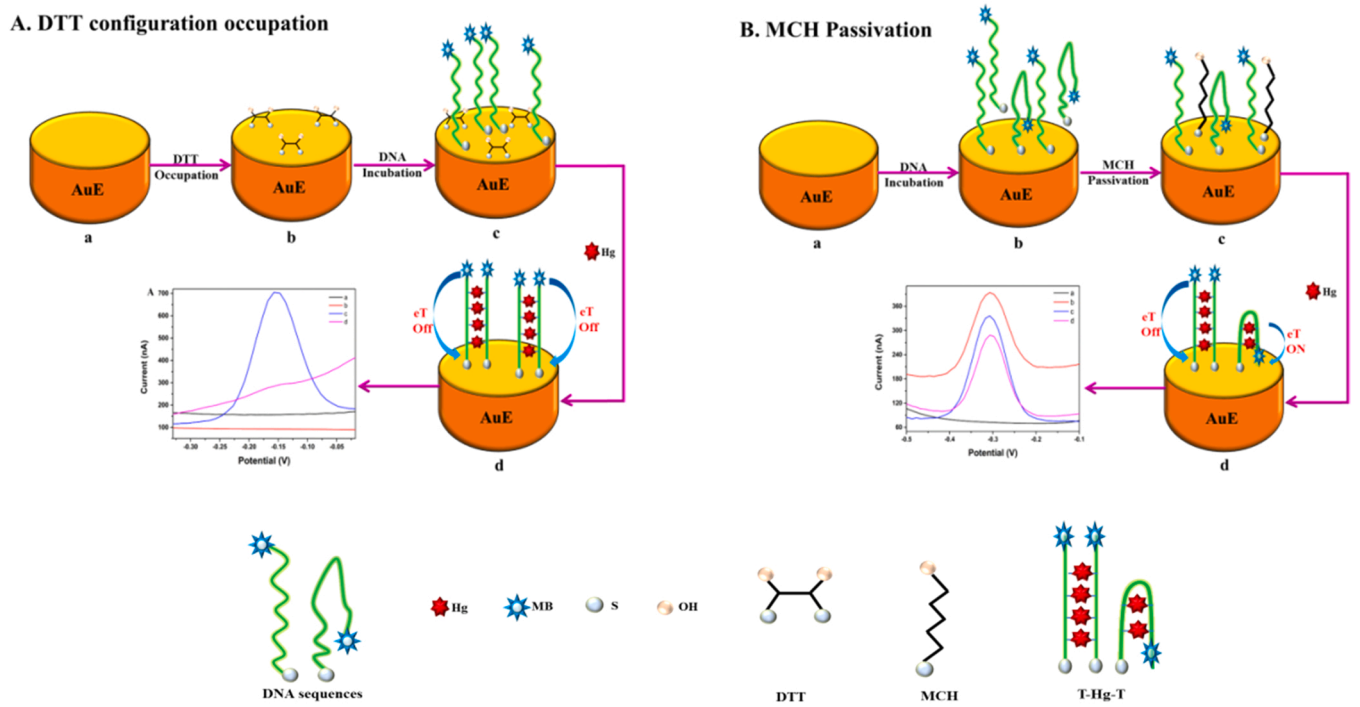

Scheme 1. Schematic illustration of the detection of Hg^{2+} based on electrochemical signal amplification by hairpin T-Hg-T structure in combination with (A) configuration occupation approach by DTT/MB-DNA/AuE and (B) passivation approach by MCH/MB-DNA/AuE.

sequence for 16 h at room temperature in dark place. Then, DTT/MB-DNA/Au electrode was obtained after carefully rinsing with ultrapure water and dried with nitrogen. For passivation approach with MCH, 10.00 μL of 1.00 μM DNA sequence was firstly incubated on AuE for 16 h to obtained MB-DNA/AuE, and then immersed in 100.00 μL 2.00 mM MCH solution for 1 h in dark place to obtain MCH/MB-DNA/ Au electrode.

2.3.2. DTT/MB-DNA/Au characterization

The optimization and characterization of DTT/MB-DNA/Au sensor was studied by SECM, CV, EIS and SWASV. SECM was performed after Z-approach test in 5.00 mmol·L^{-1} $K_3[Fe(CN)_6]$ solution (Fig. S2), and CV was performed within the potential range from - 0.20–0.60 V at 0.05 V. s^{-1}. EIS were performed in the presence of 5.00 mM $K_3[Fe(CN)_6]/K_4[Fe(CN)_6]$ in 0.10 M KCl as a redox probe in the frequency range of 0.1 Hz to 100 kHz, polarization potential of 0.15 V, and amplitude of 5.00 mV. The sensitivity and stability of DTT/MB-DNA/Au sensor was studied by SWASV in 10.00 mM PBS buffer solution containing 0.50 M NaCl, 2.70 mM KCl (pH 7.40), stripping from − 0.70–0.00 V at frequency of 50 Hz, step potential of 10 mV and amplitude of 25.00 mV.

The sensitivity was compared between DTT/MB-DNA/Au and MCH/MB-DNA/Au, and proportion of effective working area was analyzed and calculated by the Randles-Sevcik equation:

(Krukiewicz et al., 2018).

$$I_p = 2{\cdot}69\times10^5\, n^{3/2}\, AD^{1/2}\nu^{1/2}\, C \quad (1)$$

Where A is the electrode area in cm^2, D is the diffusion coefficient in $cm^2{\cdot}s^{-1}$, C is the concentration in mM, ν is the scan rate in $V{\cdot}s^{-1}$, n is the number of transferred electrons, while D is 7.60 * 10^{-6} and n is 2.

$$\text{Proportion} = \frac{A_{DTT/MB-DNA/Au}}{A_{MCH/MB-DNA/Au}}*100\% = \frac{I_{p\ AuNPs}}{I_{p\ bare\ Au}}*100\% \quad (2)$$

2.4. Electrochemical detection of Hg^{2+} by DTT/MB-DNA/Au sensor

For the detection of Hg, DTT/MB-DNA/Au sensor was immersed into 100.00 μL of sample buffer solution containing different concentration of Hg^{2+} for 1 h in dark place, followed by repeatedly cleaning the electrode surface with ultra-pure water and dried in a stream of nitrogen to remove unassembled Hg^{2+}. Then, the detection of Hg was carried out by SWASV. The limits of detection (LODs) was obtained according to the IUPAC recommended procedure for voltammetry and stripping techniques (Mocak et al., 1997), and the LODs and limits of quantification (LOQs) were calculated based on the results of 20 times' repeated experiments.

3. Result and discussion

3.1. Preparation and characterization of DTT/MB-DNA/Au sensor

3.1.1. Design and screen of DTT/MB-DNA/Au

Generally, DNA biosensors are prepared via formation of Au-S bonds, and DNA sequences can be specified as capture probe and adjunct probe (Jia et al., 2015; Zhang et al., 2018). In this work, the signal-off responsive protocols of sensor was based on architecture of T-Hg-T with two DNA single strands, in which two single strands served both as recognition element and also signaling transducer. As described in previous articles, the critical factor influencing the stability and sensitivity of the DNA biosensor cannot be ignored, was the amounts and arrange pattern, which would interfere directly with the methodology study and affect the lifetime of the sensors (Zhao et al., 2021; Chen et al., 2020; Kuralay et al., 2012). It is well known that DTT and MCH were commonly used in biosensors, as they could be competitively adsorbed onto the gold electrode via Au-S bonds, which were used to remove nonspecific aptamer adsorption on AuE surfaces (Yu et al., 2019; Wang et al., 2021a, 2021b, 2021c; Kamal et al., 2017). The main difference between MCH and DTT is that, MCH is used to remove redundant DNA sequences due to higher binding force compared to that of DNA, while DTT is based on forming a compact surface with the cyclic-(DTT) configuration backfillers to occupy the bare AuE and give a certain number of active modification sites in the subsequent DNA modification process (Wu et al., 2018; Liu et al., 2018; Wang et al., 2014).

Scheme 1 illustrated the different working mechanism of Hg with

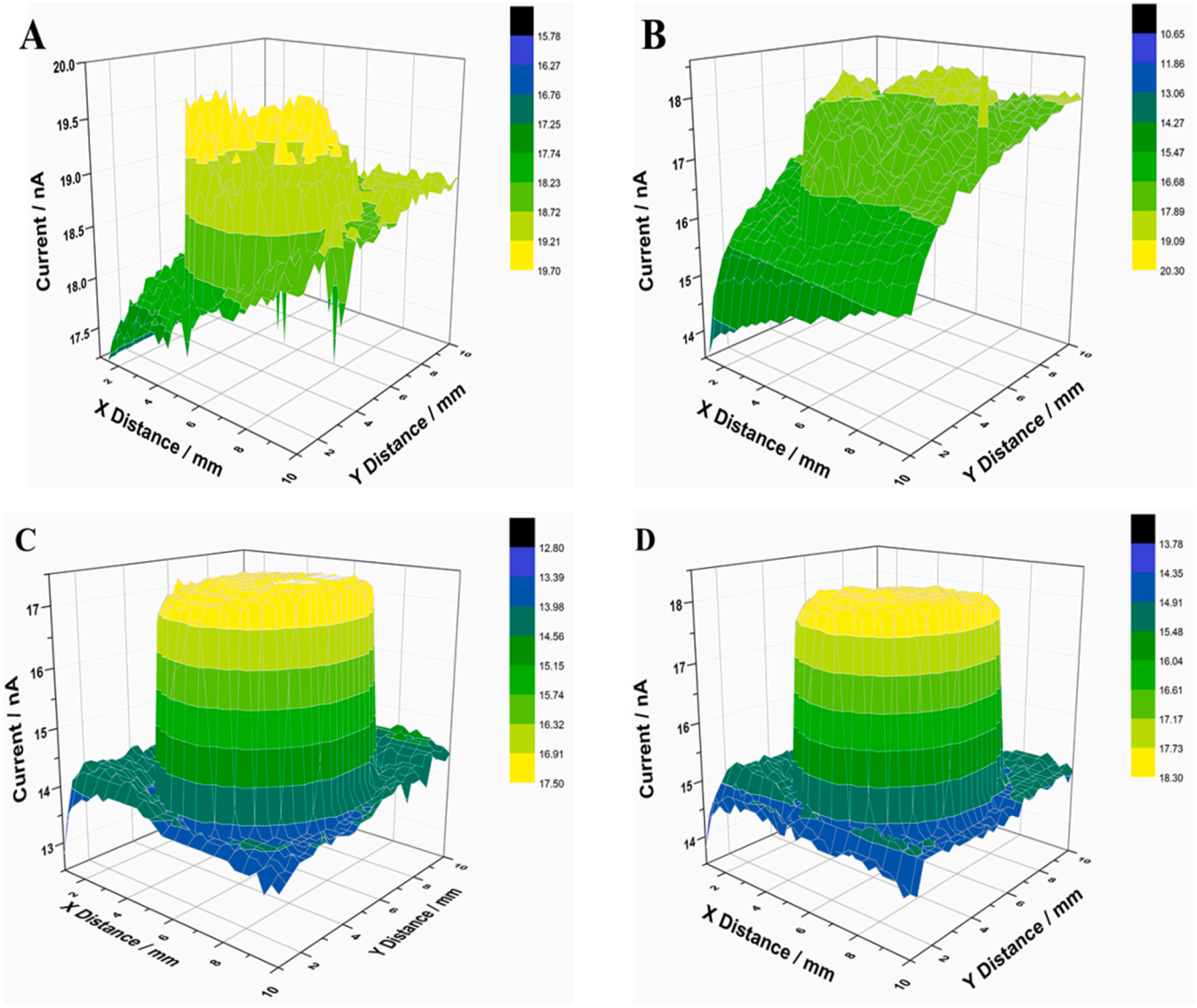

Fig. 1. Potential-based constant height mode SECM images of MCH/MB-DNA/Au (A and B) and DTT/MB-DNA/Au (C and D) tested before (A and C) and after (B and D) the detection of Hg^{2+} by using a 1.00 μm diameter Pt-UME.

different insertion approaches. Note that DTT could be stabilized by Au-S bonding to form a compact monomolecular layer on bare AuE. In the DTT approach, the SH group labeled T-rich DNA strand would insert into the limited and equally distributed positive points on DTT/AuE after the configuration occupation with DTT (Jia et al., 2015). On the other hand, if DNA is modified before MCH insertion, MCH can only be inserted into individual vacancy among the mixed and disorderly arranged DNA strands. It was worth mentioning that, in the presence of target Hg, two different T-Hg-T configurations have been formed (Wang et al., 2021a, 2021b, 2021c). As shown in Scheme 1A, due to the considerable steric hindrance with DTT layer, T-Hg-T was inclined to morph into a vertical structure between two independent adjacent DNA strands, thus leading to a signal drop due to the MB group far away from AuE surface (Wang et al., 2021a, 2021b, 2021c; Cristina et al., 2015; Long et al., 2019). In addition, in the MCH passivation approach shown in Scheme 1B, T-Hg-T can be also formed in only one DNA strand through bending the single DNA strand without monomolecular obstruction. However, the bending structure draws the MB group closer to the electrode surface, resulting in elevated signal (Kamal et al., 2017; Raju et al., 2020; Caroline et al., 2021). Therefore, in MCH passivation approach, the coexistence of vertical structure and bending structure led to the increase or decrease of alternating signal response, which made it difficult to quantitatively analyze the content of Hg with high level of reliability.

In order to further probe the relative stability between DTT/MB-DNA/Au or MCH/MB-DNA/Au has better in modification process, SECM has been adopted to conduct contrast experiments in the absence and presence of Hg^{2+}. As shown in Fig. 1, the response current amongst different spots on electrode surface of DTT/MB-DNA/Au exhibited less fluctuation than that on MCH/MB-DNA/Au, and the maximum response current difference on whole surface were 0.100 nA (Fig. 1C) and 0.700 nA (Fig. 1A). Besides, after the detection of Hg, the response current difference changed to 30.100 nA (Fig. 1D) and 10.200 nA (Fig. 1B) on DTT/MB-DNA/Au and MCH/MB-DNA/Au, respectively. Moreover, before and after the detection of Hg (Table S1), the average relative current change value of DTT insertion approach was 97.607% with high reproducibility (RSD = 0.223%, $n \geq 10$), while of MCH blocking approach was only 57.518% but with low repeatability (RSD = 22.658%, $n \geq 10$). In addition, according to the Randles-Sevcik equation (Formula 1 and Formula 2), the increased proportion of effective working area of DTT/MB-DNA/Au was 467.380% compared to that of MCH/MB-DNA/Au (Krukiewicz et al., 2018). Thus, the superiority of DTT/MB-DNA/Au on stability and sensitivity has been proven by

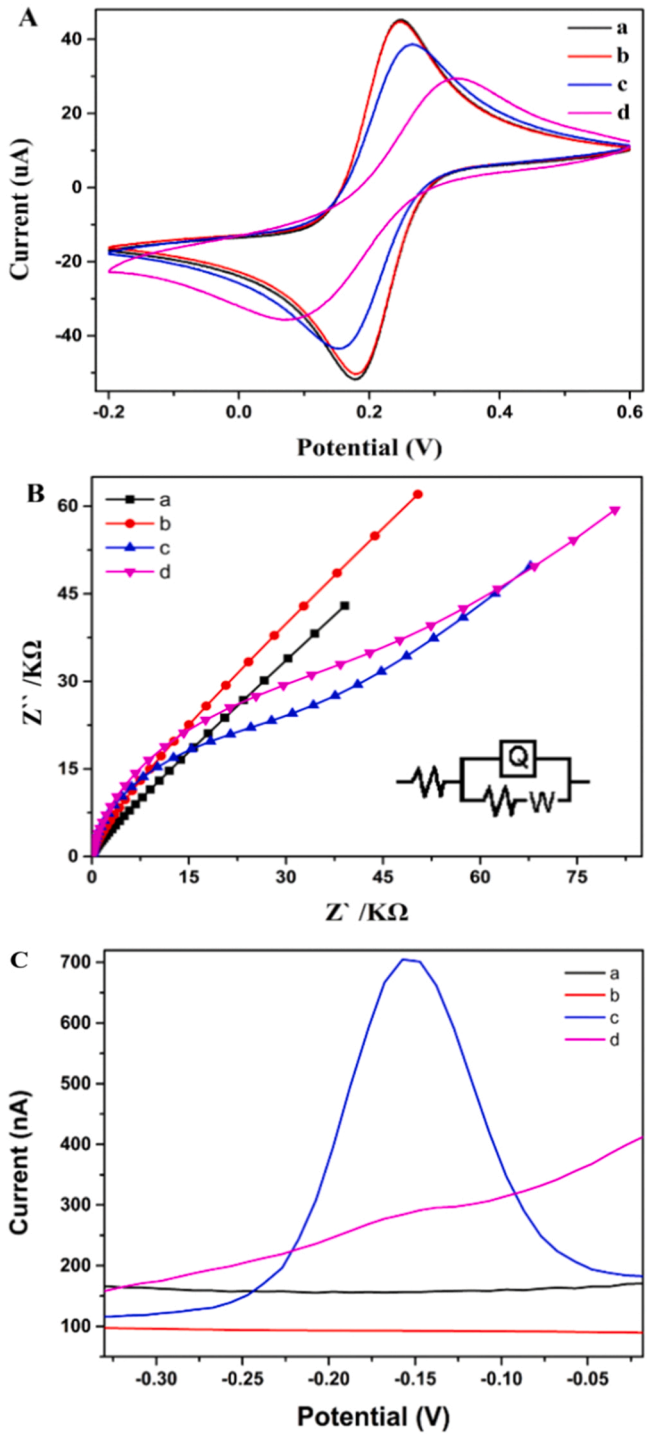

Fig. 2. The graphs of CV (A), EIS (B) and SWSV (C) tested in the solution of 5.00 mmol·L^{-1} $K_3[Fe(CN)_6]$. a) bare AuE, b) after insertion with DTT 30 min, c) after modification with MB-DNA on DTT/AuE for 16 h, d) after immerse in the solution of 5.00 umol·L^{-1} Hg^{2+} on DTT/ MB-DNA/AuE.

theoretical analysis as well as experiment evidence. As such, DTT/MB-DNA/Au will be further developed in the following optimization and detection experiments.

3.1.2. *Characterization of DTT/MB-DNA/Au*

In addition to SECM technique, CV and EIS are also rather useful and efficient tools for characterizing the interface structure of sensor in different stages, before and after DNA modification (Varmira et al., 2018; Park et al., 2020). As shown in Fig. 2, the preparation and detection process of DTT/MB-DNA/Au was characterized by CV, EIS and SWSV, which contained bare AuE, AuE inserted with DTT, the assembled DTT-DNA, and the detection of Hg on DTT/MB-DNA/Au. It is worth noticing that when compared with the bare AuE and DTT covered AuE (Fig. 2Aa, Ab), thiolate DNA-modified electrode (Fig. 2Ac) showed a marked oxidation peak current decreased at the potential of 0.20 V in CV test. This is attributed to the electrostatic repulsion between the DNA strands and DTT, and the results of EIS (Fig. 2B) are in line with CV measurements. Moreover, in SWASV test, the current intensity of baseline was decreased and tended to be smooth after the addition of DTT on bare AuE, indicating that DTT covers the AuE surface evenly and forms a semi conductive sealing film. While, the oxidation peak of − 0.165 V appeared after MB-DNA incubated on DTT-AuE (Fig. 2Cb), indicating that the DNA strand was successfully assembled and formed the DTT/MB-DNA/Au. Then, the current signals of MB-DNA probe electrode (Fig. 2Cc) were reduced significantly after adding the standard solution of Hg (Fig. 2Cd), the current of oxidation peak of DTT/MB-DNA/Au can reach as high as 558.800 nA, while the T-Hg-T probe peak current decreased to 12.040 nA. This could be attributed to the formation of a dense, non-conducting DNA layer on the surface of the Au electrode after the formation of T-Hg-T, which hinders the transmission of electrons on the surface of the electrode.

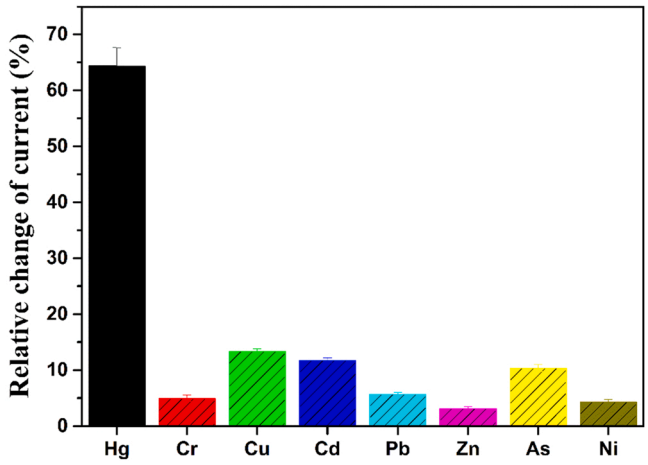

Fig. 3. Selectivity of the DTT/MB-DNA/Au for Hg^{2+} determination by SWASV. The concentration of all interfering elements was 1.00 μM, and that of Hg was 0.25 μM.

3.2. *Optimization of experiment conditions*

According to the relevant articles, the modification procedure has strong correlation with signal amplification ability (Jia et al., 2015; Sun et al., 2010; Kong et al., 2020). So, in order to improve the stability, sensitivity and anti-interference ability of the single strand DNA electrochemical biosensor in the Hg detection application, researchers have carefully investigated several critical parameters in modification processes, including the DTT concentration, MB-DNA strands concentration and DNA assembly time. It can be inferred from Fig. S3A that, the peak current signal had increased with the increasing of DTT concentration with an optimum value of 100.00 μmol·L^{-1}. Therefore, 100.00 μmol·L^{-1} DTT was used in electrode configuration occupation. Besides, at MB-DNA concentration of 1.00 μmol·L^{-1}, an SWSV peak value of 705.218 nA can be achieved with a low RSD of 2.494% (Fig. S3B). It has also been observed that, high sensitivity and stability were both obtained under the assembly time of 16 h (Fig. S3C). Thus, DTT/MB-DNA/Au was preferably prepared under the DTT concentration of 100.00 μmol·L^{-1} with assembling 1.00 μmol·L^{-1}MB-DNA for 16 h.

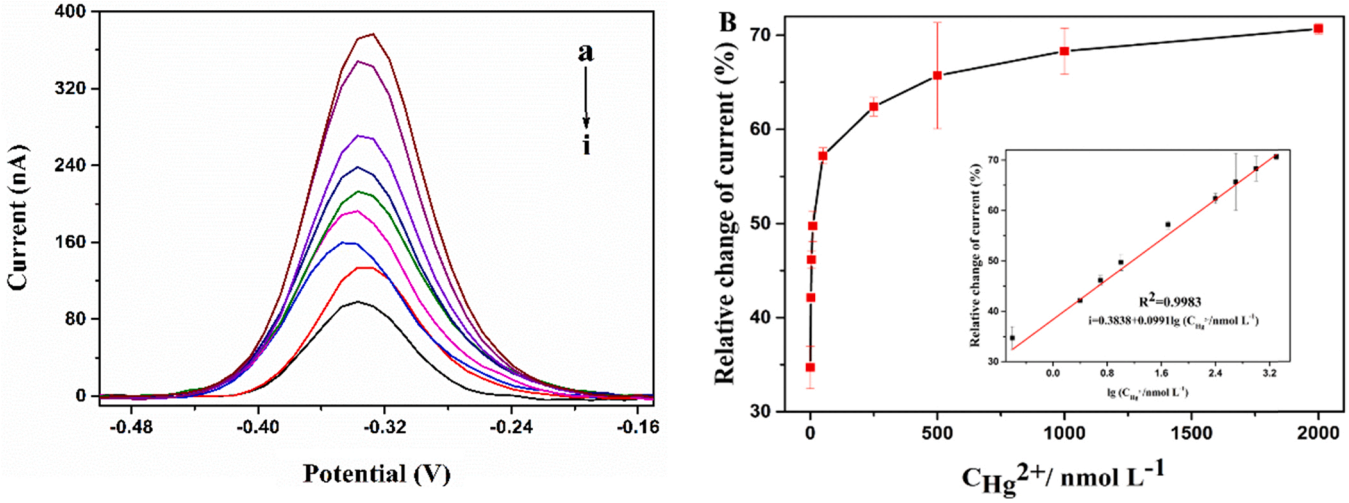

Fig. 4. SWASV curves (A) and calibration curve (B) measured in buffer solution with different concentrations of Hg. a) 0.25 nM, b) 2.50 nM, c) 5.00 nM, d) 10.00 nM, e) 50.00 nM, f) 250.00 nM, g) 500.00 nM, h) 1.00 μM, i) 2.00 μM. Error bars represented the standard deviation of three replicates from one electrode.

3.3. Method validation

3.3.1. Selectivity and stability of DTT/MB-DNA/Au

To investigate the selectivity of the proposed DTT/MB-DNA/Au, a series of commonly existing toxic elements were studied, including Cr^{3+}, Cu^{2+}, Cd^{2+}, Pb^{2+}, Zn^{2+}, $As^{3+}$and Ni^{2+} (each 1.00 μM) under optimum conditions. Fig. 3 described the relative current changes of SWASV responses with DTT/MB-DNA/Au, to the series of seven elements. As was expected, even micromole concentrations of typical metal ions exhibited much weaker relative current responses than Hg^{2+} at nM level. Therefore, the optimized DTT/MB-DNA/Au has an excellent selectivity for Hg^{2+} against other environment or food related elements. The good performance in selectivity is mainly attributed to the specific coordination between T bases and Hg^{2+}.

The stability was evaluated by injecting and analyzing the Hg at 1, 2, 3, 4, 5, 6 and 7 days under the same condition. As shown in Fig. S4 and Table S2, the peak current signal value decreased from 645.404 nA to 278.209 nA after 7 days. Moreover, the relative current change value was only 2.434% within 3 days, so it was indicated that the optimized DTT/MB-DNA/Au was satisfactory regarding stability within 3 days.

3.3.2. Linearity, LOQ and LOD

Under the optimized experimental conditions, a series of DTT/MB-DNA/Au electrodes were immersed and incubation with different concentrations of Hg for 1 h, and the test result was shown in Fig. 4. The peak current signal values were decreased with the increasing of Hg concentration. The relative peak current changes against the logarithm of Hg^{2+} concentration was linear over the range from 0.250 nM to 2.00 μM ($i = 0.384 + 0.099\ \lg(C_{Hg2+}/\text{nmol L}^{-1})$) with a detection limit of 53.000 pM based on a signal three-fold the background noise. Such a low detection limit is much lower than the International Standard Organization standard (0.50–2.50 μM of Hg^{2+} for medicinal plant and Chinese medicinal material) (International standard organization, 2015). Therefore, the analytical performance indicated that the proposed DTT/MB-DNA/Au can be applied in the determination of trace level Hg in natural plants samples.

3.4. Application in commercial medicine samples

3.4.1. Practical application in plants and food related samples

To evaluate whether this optimized DTT/MB-DNA/Au is applicable to natural and medicinal samples, the recoveries of added Hg^{2+} in plants and medicinal samples were determined, including Astragalus membranaceus, Cassia stem and a regular medicinal formulation decoction. The recovery results obtained by spiked with the Hg standard solution into medicinal sample powders before digestion, in triplicate and at three different concentration percent levels (0.5, 1.0, and 2.0 times of the original content of Hg in sample). And as were shown in Table S3, and it could be observed that the found values were extremely close to the added values. Besides, the recovery of Hg^{2+} of plant samples was

Table 1
The detection performance comparison of sensors in analysis of Hg in recent published articles.

No.	Sensor	Sample type	Linear range	LOD	Repeatability (RSD %)	Year
1	T-Hg-T and exonuclease III	water	1.00 pM - 1.00 μM	0.22 pM	0.34 (n = 3)	(Wang et al., 2021a, 2021b, 2021c)
2	Thioctic acid-carbon dots	water	0.05 μM - 5.00 μM	8.00 nM	ND[a]	(Wang et al., 2021a, 2021b, 2021c)
3	DNA-assembled graphene oxide	water	0.12–50.00 nM	0.12 nM	9.60% (n = 3)	(Lu et al., 2016)
4	RTIL/γAlOOH/Fe(OH)3 composite	soil	5.00 nM - 0.40 μM	0.50 nM	3.90% (n = 5)	(Zhang et al., 2018)
5	Ag-dopped reduced graphene oxide	fish	0.05 nM - 0.50 μM	24.50 pM	3.55% (n = 5)	(Ma et al., 2021)
6	Au/AuE	bombyx batryticatus	0.05 μM - 0.50 μM	17.50 nM	2.59 (n = 20)	(Yan et al., 2020)
7	Au nano particles system	marine products	0.10 μM - 0.50 mM	37.75 nM	2.87 (n ≤ 20)	(Kong et al., 2020)
8	Pt-doped $NiCo_2O_4$ nanograss	water	0.50 nM - 0.60 μM	0.25 nM	2.35 (n = 15)	(Zahra et al., 2022)
9	N, $PTi_3C_2T_xR$/GCE	tap water and lake water	5.00 nM - 2.50 μM	0.29 nM	3.37 (n = 8)	(Xia et al., 2022)
10	Fe_2O_3/Mn_3O_4 nanocubes	water	0.20 μM - 1.20 μM	1.39 nM	2.10 (n = 10)	(Li et al., 2021)
11	DTT/MB-DNA/Au	plants and medicinal formulations	0.25 nM - 2.00 μM	53.00 pM	0.23 (n = 3) 2.43 (n = 10)	**This work**

[a] ND: Not described.

achieved in the range of 93.580–115.650% and of medicinal formulation was of 89.290–113.480%, which was in good agreement with the performance criteria requirements. Thus, it was demonstrated that the proposed DTT/MB-DNA/Au has feasibility in real natural and food-related samples.

3.4.2. Comparison of DTT/MB-DNA/Au with other sensors in complex samples

To further prove the superiority of the proposed techniques and DTT/MB-DNA/Au, a comparison of analytical performance between the published studies and DTT/MB-DNA/Au for Hg detection was concluded in Table 1, including the linear detection range, detection limit and repeatability. It was worth mentioning that few articles have been used to analyze Hg in plants and medicinal samples, and compared with different sample matrix, the wide detection range and repeatability (RSD) of DTT/MB-DNA/Au are much superior to that of reported sensors. Hence, the optimized DTT/MB-DNA/Au combining with SWASV can be promising for fast screening of trace Hg in complex plants and medicinal samples.

4. Conclusion

In this study, a stable and sensitive screening system was established through the design, preparation, optimization, characterization and application of DTT/MB-DNA/Au in plants and medicinal formulation samples. Two different assembly approaches were compared between DTT configuration occupation method and MCH passivation method. Combining SECM-based electrochemical experiments and theoretical calculations by Randles-Sevcik equation, it was demonstrated that the stability and sensitivity of as-prepared DTT/MB-DNA/Au was higher than any other fast screening system, especially when probing complex matrix samples. Besides, after the optimization of experiments condition by CV, EIS and SWASV, the DTT/MB-DNA/Au showed a low LOD of 53.00 pM and a wide liner range from 0.25 nM to 2.00 μM. Moreover, this sensor has been applied into evaluating the trace Hg in two plants and a medicinal formulation with satisfactory results, ensuring the potential for selective detection of Hg in food and medicinal-related industries. More significantly, the stability and lifetime of DTT/MB-DNA/Au were at least two times better than analogous previously reported sensors, even after 3 days under room temperature. Accordingly, this optimized DTT/MB-DNA/Au with advantages of high reproducibility and sensitivity would provide a new insight into the design and application of biosensor for reliable sensing in safeguarding plants protection and medicinel safety.

CRediT authorship contribution statement

Dandan Kong, Meihua Yang: Funding acquisition, Conceptualization, methodology, Data curation, Paper writing. **Xinyue Li, Yang Tang, Ming Sui, Gaofeng Wang, Wei Gu, Xuegang Guo**: Investigation, Methodology, Paper writing. **Dandan Kong, Meihua Yang, Jinping Li, Yonggui Ma**: Project administration, Resources, Supervision.

Declaration of Competing Interest

The authors declare that they have no known competing financial interests or personal relationships that could have appeared to influence the work reported in this paper.

Acknowledgement

This work was financially supported by the National Natural Science Foundation of China, China (No. 81903797), CAMS Innovation Fund for Medical Science (CIFMS), Chinese Academy of Medical Sciences, China (No. 2021-I2M-1–031, 2021-I2M-1–071).

Appendix A. Supporting information

Supplementary data associated with this article can be found in the online version at doi:10.1016/j.ecoenv.2022.113391.

References

Ajjabi, L.C., Chouba, L., 2009. Biosorption of $Cu^{(2+)}$ and $Zn^{(2+)}$ from aqueous solutions by dried marine green macroalga Chaetomorpha linum. J. Environ. Manag. 90 (11), 3485–3489. https://doi.org/10.1016/j.jenvman.2009.06.001.

Bonciu, A., Vasilescu, A., Dinca, V., Peteu, S.F., 2021. Interfaces obtained by MAPLE for chemical and biosensors applications. Sens. Actuators Rep. 100040 (3) https://doi.org/10.1016/j.snr.2021.100040.

Caroline, G.S., Rafael, M.B., Raphael, P.B., Iranaldo, S.D.S., Adriana, D.R., Fernanda, P. C., Silvia, H.P.S., 2021. Sensing materials: electrochemical applications of DNA sensors and biosensors. Ref. Modul. Biomed. Sci. https://doi.org/10.1016/B978-0-12-822548-6.00039-X.

Clarkson, T.W., Magos, L., 2006. The toxicology of mercury and its chemical compounds. Crit. Rev. Toxicol. 36 (8), 609–662. https://doi.org/10.1080/10408440600845619.

Dmitry, T., Ilya, V., Anna, V., Margarita, M., Alexander, T., Elena, Alexander, M., Valentin, O., 2022. The chemical state of Hg in synthetic crystals of zinc and mercury sulfides studied by XAFS spectroscopy. J. Solid State Chem. 305, 122708 https://doi.org/10.1016/j.jssc.2021.122708.

Do Nascimento, F.H., Masini, J.C., 2012. Complexation of Hg(II) by humic acid studied by square wave stripping voltammetry at screen-printed gold electrodes. Talanta 100, 57–63. https://doi.org/10.1016/j.talanta.2012.08.018.

Elisabeth, M., Terry, M., Azad, M., 2018. Optimization of instrument conditions for the analysis for mercury, arsenic, antimony and selenium by atomic absorption spectroscopy. MethodsX 5, 824–833. https://doi.org/10.1016/j.mex.2018.07.016.

Fernanda, C., Diego, V., Ariane, I., Edenir, R., Joaquim, A., 2019. Microwave-assisted digestion using dilute nitric acid solution and investigation of calibration strategies for determination of As, Cd, Hg and Pb in dietary supplements using ICP-MS. J. Pharm. Biomed. Anal. 174, 471–478. https://doi.org/10.1016/j.jpba.2019.06.018.

Fitzgerald, W.F., Lamborg, C.H., Hammerschmidt, C.R., 2007. Marine biogeochemical cycling of mercury. Chem. Rev. 107 (2), 641–662. https://doi.org/10.1021/cr050353m.

García-Seoane, R., Fernández, J.A., Varela, Z., Real, C., Boquete, M.T., Aboal, J.R., 2019. Sampling optimization for biomonitoring metal contamination with marine macroalgae (Barking, Essex: 1987). Environ. Pollut. 255 (Pt 3), 113349. https://doi.org/10.1016/j.envpol.2019.113349.

Hai, X., Li, Y.F., Zhu, Zhu, C.Z., Song, W.L., Cao, J.Y., Bi, S., 2020. Dna-based label-free electrochemical biosensors: from principles to applications. TrAC Trends Anal. Chem. 133 (2), 116098 https://doi.org/10.1016/j.trac.2020.116098.

He, L.L., Cheng, L., Lin, Y., Cui, H.F., Hong, N., Peng, H., Fan, H., 2018. A sensitive biosensor for mercury ions detection based on hairpin hindrance by thymine-Hg(II)-thymine structure. J. Electroanal. Chem. 814, 161–167 https://doi-org.libproxy.library.unt.edu/10.1016/j.jelechem.2018.02.050.

Henstridge, M.C., Laborda, E., Dickinson, E.J., Compton, R.G., 2012. Redox systems obeying Marcus–Hush–Chidsey electrode kinetics do not obey the Randles–Ševčík equation for linear sweep voltammetry. J. Electroanal. Chem. 664, 73–79. https://doi.org/10.1016/j.jelechem.2011.10.015.

Himori, S., Nishitani, S., Sakata, T., 2021. Aptamer-based nanofilter interface for small-biomarker detection with potentiometric biosensor. Electrochim. Acta 368, 137631. https://doi.org/10.1016/j.electacta.2020.137631.

International standard organization, 2015, ISO 18664: Traditional Chinese Medicine-Determination of heavy metals in herbal medicines used in Traditional Chinese Medicine. Switzerland.

Jia, J., Ling, Y., Gao, Z.F., Lei, J.L., Luo, H.Q., Li, N.B., 2015. A regenerative electrochemical biosensor for mercury(II) by using the insertion approach and dual-hairpin-based amplification. J. Hazard. Mater. 295, 63–69. https://doi.org/10.1016/j.jhazmat.2015.04.017.

Kamal, A., She, Z., Sharma, R., Kraatz, H.B., 2017. A study of the interactions of Hg(II) with TT mispair containing hairpin loops. Electrochim. Acta 243, 44–52 https://doi-org.libproxy.library.unt.edu/10.1016/j.electacta.2017.05.058.

Kong, D., Yao, J., Li, X., Luo, J., Yang, M., 2020. A reusable AuNPS with increased stability applied for fast screening of trace heavy metals in edible and medicinal marine products. Ecotoxicol. Environ. Saf. 204, 111107 https://doi.org/10.1016/j.ecoenv.2020.111107.

Konstantin, A., Mikhail, A., Alexander, V., Zaual, A., Mikhail, Y., Karina, A., 2018. A novel photochemical vapor generator for ICP-MS determination of As, Bi, Hg, Sb, Se and Te. Talanta 187, 370–378. https://doi.org/10.1016/j.talanta.2018.05.052.

Krukiewicz, K., Krzywiecki, M., Biggs, M., Janas, D., 2018. Chirality-sorted carbon nanotube films as high capacity electrode materials. RSC Adv. 8, 30600–30609. https://doi.org/10.1039/C8RA03963A.

Kuralay, F., Campuzano, S., Wang, J., 2012. Greatly extended storage stability of electrochemical DNA biosensors using ternary thiolated self-assembled monolayers. Talanta 99, 155–160. https://doi.org/10.1016/j.talanta.2012.05.033.

Li, F., Xu, L., You, T., Lu, A., 2021. Measurement of potentially toxic elements in the soil through NIR, MIR, and XRF spectral data fusion. Comput. Electron. Agric. 187, 106257 https://doi.org/10.1016/j.compag.2021.106257.

Li, J., Zhuang, Z., Guo, Z., Liu, Z., Huang, X., 2021. Framework-derived Fe_2O_3/Mn_3O_4 nanocubes as electrochemical catalyst for simultaneous analysis of Cu(II) and Hg(II). Electrochim. Acta 399, 139412. https://doi.org/10.1016/j.electacta.2021.139412.

Liang, P., Wu, S.C., Zhang, C., Zhang, J., Wong, M.H., 2021. Environmental geochemistry of Hg in intensive fish farming sites: implications of Hg speciation change related to its health perspectives. Curr. Opin. Environ. Sci. Health, 100242. https://doi.org/10.1016/j.coesh.2021.100242.

Liu, H., Wang, J., Jin, H., Wei, M., Ren, W., Zhang, Y., He, B., 2021. Electrochemical biosensor for sensitive detection of Hg^{2+} baesd on clustered peonylike copper-based metal-organic frameworks and DNAzyme-driven DNA Walker dual amplification signal strategy. Sens. Actuators B: Chem. 329, 129215 https://doi.org/10.1016/j.snb.2020.129215.

Liu, H., Wang, J.S., Jin, H.L., Wei, M., Ren, W.J., Zhang, Y.R., Wu, L.G., He, B.S., 2020. Electrochemical biosensor for sensitive detection of Hg^{2+} baesd on clustered peonylike copper-based metal-organic frameworks and dnazyme-driven dna walker dual amplification signal strategy. Sens. Actuators B: Chem. 329 (15), 129215 https://doi.org/10.1016/j.snb.2020.129215.

Liu, W., Wang, X., Wang, Y., Li, J., Shen, D., Kang, Q., Chen, L., 2018. Ratiometric fluorescence sensor based on dithiothreitol modified carbon dots-gold nanoclusters for the sensitive detection of mercury ions in water samples. Sens. Actuators B: Chem. 262, 810–817. https://doi.org/10.1016/j.snb.2018.01.222.

Long, D., Li, M., Wang, H., Wang, H., Chai, Y., Yuan, R., 2019. A photoelectrochemical biosensor based on fullerene with methylene blue as a sensitizer for ultrasensitive DNA detection. Biosens. Bioelectron. 142, 111579 https://doi.org/10.1016/j.bios.2019.111579.

Lu, M., Xiao, R., Zhang, X., Niu, J., Zhang, X., Wang, Y., 2016. Novel electrochemical sensing platform for quantitative monitoring of Hg(II) on DNA-assembled graphene oxide with target recycling. Biosens. Bioelectron. 85, 267–271. https://doi.org/10.1016/j.bios.2016.05.027.

Ma, S., Zhang, Q., Zhu, J., Shi, H., Zhang, K., Shen, Y., 2021. Rational engineering of Ag-dopped reduced graphene oxide as electrochemical sensor for trace mercury ions monitoring. Sens. Actuators B: Chem., 130383. https://doi-org.libproxy.library.unt.edu/10.1016/j.snb.2021.130383.

Marinho, O.R., Kamogawa, M.Y., Ferreira, J.R., Reis, B.F., 2020. Automated liquid–liquid extraction procedure for the photometric determination of nanogram levels of Hg(II) in soil and sediment extracts. Microchem. J. 156, 104978 https://doi.org/10.1016/j.microc.2020.104978.

Martinis, E.M., Wuilloud, R.G., 2016. Enhanced spectrophotometric detection of Hg in water samples by surface plasmon resonance of Au nanoparticles after preconcentration with vortex-assisted liquid-liquid microextraction. Spectrochim. Acta Part A, Mol. Biomol. Spectrosc. 167, 111–115. https://doi.org/10.1016/j.saa.2016.05.028.

Meng, Y., Kong, D., Wang, R., Kong, W., Fan, Z., Huang, Y., Yang, M., 2017. Electrochemical co-detection of heavy metals in Astragalus Membranaceus by anodic stripping voltammetry. Int. J. Electrochem. Sci. 12 (9), 8106–8119. https://doi.org/10.20964/2017.09.19.

Mocak, J., Bond, A.M., Mitchell, S., Scollary, G., 1997. A statistical overview of standard (IUPAC and ACS) and new procedures for determining the limits of detection and quantification: application to voltammetric and stripping techniques (technical report). Pure Appl. Chem. 69 (2), 297–328 https://doi-org.libproxy.library.unt.edu/10.1351/pac199769020297.

Park, S.Y., Kim, J., Yim, G., Jang, H., Lee, Y., Kim, S.M., Park, C., Lee, M.H., Lee, T., 2020. Fabrication of electrochemical biosensor composed of multi-functional DNA/rhodium nanoplate heterolayer for thyroxine detection in clinical sample (Advance online publication). Colloids Surf. B, Biointerfaces 195, 111240. https://doi.org/10.1016/j.colsurfb.2020.111240.

Pinheiro, F.C., Babos, D.V., Barros, A.I., Pereira-Filho, E.R., Nóbrega, J.A., 2019. Microwave-assisted digestion using dilute nitric acid solution and investigation of calibration strategies for determination of As, Cd, Hg and Pb in dietary supplements using ICP-MS. J. Pharm. Biomed. Anal. 174, 471–478. https://doi.org/10.1016/j.jpba.2019.06.018.

Raju, V.M., Bhavana, V., Gayathri, G.K., Suryan, S., Reddy, R., Reddy, N., Santosh, M.S., 2020. A novel disposable electrochemical DNA biosensor for the rapid detection of Bacillus thuringiensis. Microchem. J. 159, 105434 https://doi.org/10.1016/j.microc.2020.105434.

Sun, C., Zhang, L., Jiang, J., Shen, G., Yu, R., 2010. Electrochemical DNA biosensor based on proximity-dependent DNA ligation assays with DNAzyme amplification of hairpin substrate signal. Biosens. Bioelectron. 25 (11), 2483–2489. https://doi.org/10.1016/j.bios.2010.04.012.

Tamara, F., Beatriz, G., Roberto, P., Emma, G., Teresa, P., Yolanda, M., 2022. Analysis of Se and Hg biomolecules distribution and Se speciation in poorly studied protein fractions of muscle tissues of highly consumed fishes by SEC-UV-ICP-MS and HPLC-ESI-MS/MS. Talanta 237, 122922. https://doi.org/10.1016/j.talanta.2021.122922.

Timmaraju, K., Fajurally, B., Armstrong, A., Chettle, D., 2016. Development of a 170Tm source for mercury monitoring studies in humans using XRF. Appl. Radiat. Isot. 110, 70–73. https://doi.org/10.1016/j.apradiso.2015.12.066.

Varmira, K., Abdi, O., Gholivand, M.B., Goicoechea, H.C., Jalalvand, A.R., 2018. Intellectual modifying a bare glassy carbon electrode to fabricate a novel and ultrasensitive electrochemical biosensor: Application to determination of acrylamide in food samples. Talanta 176, 509–517. https://doi.org/10.1016/j.talanta.2017.08.069.

Wang, Q., Zhou, Q., Zhang, Q., Shi, R., Ma, S., Zhao, W., Zhou, M., 2018a. Fabrication of novel superoxide anion biosensor based on 3D interface of mussel-inspired Fe_3O_4-$Mn_3(PO_3)_2$@Ni foam. Talanta 179, 145–152. https://doi.org/10.1016/j.talanta.2017.10.054.

Wang, R., Kong, D., Yao, J., Dou, X., Huang, Y., Yang, S., Yang, M., 2018b. A BiFEs-based SWASV method for fast screening of multi-heavy metals in Xiaochaihu Tang. Microchem. J. 143, 319–325. https://doi.org/10.1016/j.microc.2018.08.026.

Wang, S., Chen, H., Xie, H., Wei, L., Xu, L., Zhang, L., Lan, W., Zhou, C., She, Y., Fu, H., 2021a. A novel thioctic acid-carbon dots fluorescence sensor for the detection of Hg^{2+} and thiophanate methyl via S-Hg affinity. Food Chem. 346, 128923 https://doi.org/10.1016/j.foodchem.2020.128923.

Wang, X., Xu, C.F., Wang, Y.X., Li, W., Chen, Z.B., 2021b. Electrochemical DNA sensor based on T-Hg-T pairs and exonuclease III for sensitive detection of Hg^{2+}. Sens. Actuators B Chem. 343, 130151 https://doi.org/10.1016/j.snb.2021.130151.

Wang, Y., Feng, J., Tan, Z., Wang, H., 2014. Electrochemical impedance spectroscopy aptasensor for ultrasensitive detection of adenosine with dual backfillers. Biosens. Bioelectron. 60, 218–223. https://doi.org/10.1016/j.bios.2014.04.022.

Wang, Y.M., Li, L.J., Yao, C., Tian, X.S., Wu, Y.R., Xie, Q., Wang, D.Y., 2021c. Mercury in human hair and its implications for health investigation. Curr. Opin. Environ. Sci. Health 22, 100271. https://doi.org/10.1016/j.coesh.2021.100271.

Wu, S.H., Zhang, B., Wang, F.F., Mi, Z.Z., Sun, J.J., 2018. Heating enhanced sensitive and selective electrochemical detection of Hg^{2+} based on T-Hg^{2+}-T structure and exonuclease III-assisted target recycling amplification strategy at heated gold disk electrode. Biosens. Bioelectron. 104, 145–151. https://doi.org/10.1016/j.bios.2018.01.004.

Xia, Y., Zhao, Y., Ai, F., Yi, Y., Liu, T., Lin, H., Zhu, G., 2022. N and P co-doped MXenes nanoribbons for electrodeposition-free stripping analysis of Cu(II) and Hg(II). J. Hazard. Mater. 425, 127974 https://doi.org/10.1016/j.jhazmat.2021.127974.

Yan, H., Kong, D., Li, X., Luo, J., Fan, Z., Yang, M., 2020. Multi-channel electroanalysis of As (III), Hg and Cu in the complex matrix of Bombyx batryticatus after pre-purification. Microchem. J. 155, 104707 https://doi.org/10.1016/j.microc.2020.104707.

Yu, Y., Yu, C., Gao, R., Chen, J., Zhong, H., Wen, Y., Ji, X., Wu, J., He, J., 2019. Dandelion-like CuO microspheres decorated with Au nanoparticle modified biosensor for Hg^{2+} detection using a T-Hg^{2+}-T triggered hybridization chain reaction amplification strategy. Biosens. Bioelectron. 131, 207–213. https://doi.org/10.1016/j.bios.2019.01.063.

Zahra, G., Hamid, A., Hadi, M., 2022. An efficient sensor for simultaneous determination of Hg (II) and As (III) using a carbon paste electrode modified with needle-shaped Pt-doped $NiCo_2O_4$ nanograss. Sens. Actuators B: Chem. 358, 131445 https://doi.org/10.1016/j.snb.2022.131445.

Zhang, Y., Wang, Q., Xie, F., Xiong, S., 2018. The stripping analysis of Hg (II) and Cu (II) based on hierarchical RTIL/γ-AlOOH/$Fe(OH)_3$ composite. Electrochim. Acta 287, 87–95 https://doi-org.libproxy.library.unt.edu/10.1016/j.electacta.2018.08.020.

Zhang, Z.H., Fu, X.M., Li, K.Z., Liu, R.X., Peng, D.L., He, L.H., Wang, M.H., Zhang, H.Z., Zhou, L.M., 2016. One-step fabrication of electrochemical biosensor based on dna-modified three-dimensional reduced graphene oxide and chitosan nanocomposite for highly sensitive detection of hg(II). Sensors and Actuators. B. Chem. 225 (31), 453–462. https://doi.org/10.1016/j.snb.2015.11.091.

Zhao, S., Liu, N., Wang, W., Xu, Z., Wu, Y., Luo, X., 2021. An electrochemical biosensor for alpha-fetoprotein detection in human serum based on peptides containing isomer D-Amino acids with enhanced stability and antifouling property. Biosens. Bioelectron. 190, 113466 https://doi.org/10.1016/j.bios.2021.113466.

Zhou, Y., Li, Y.S., Meng, X.Y., Zhang, Y.Y., Yang, L., Zhang, J.H., 2013. Development of an immunochromatographic strip and its application in the simultaneous determination of hg(II), cd(II) and pb(II). Sens. Actuators B Chem. 183 (5), 303–309. https://doi.org/10.1016/j.snb.2013.04.028.